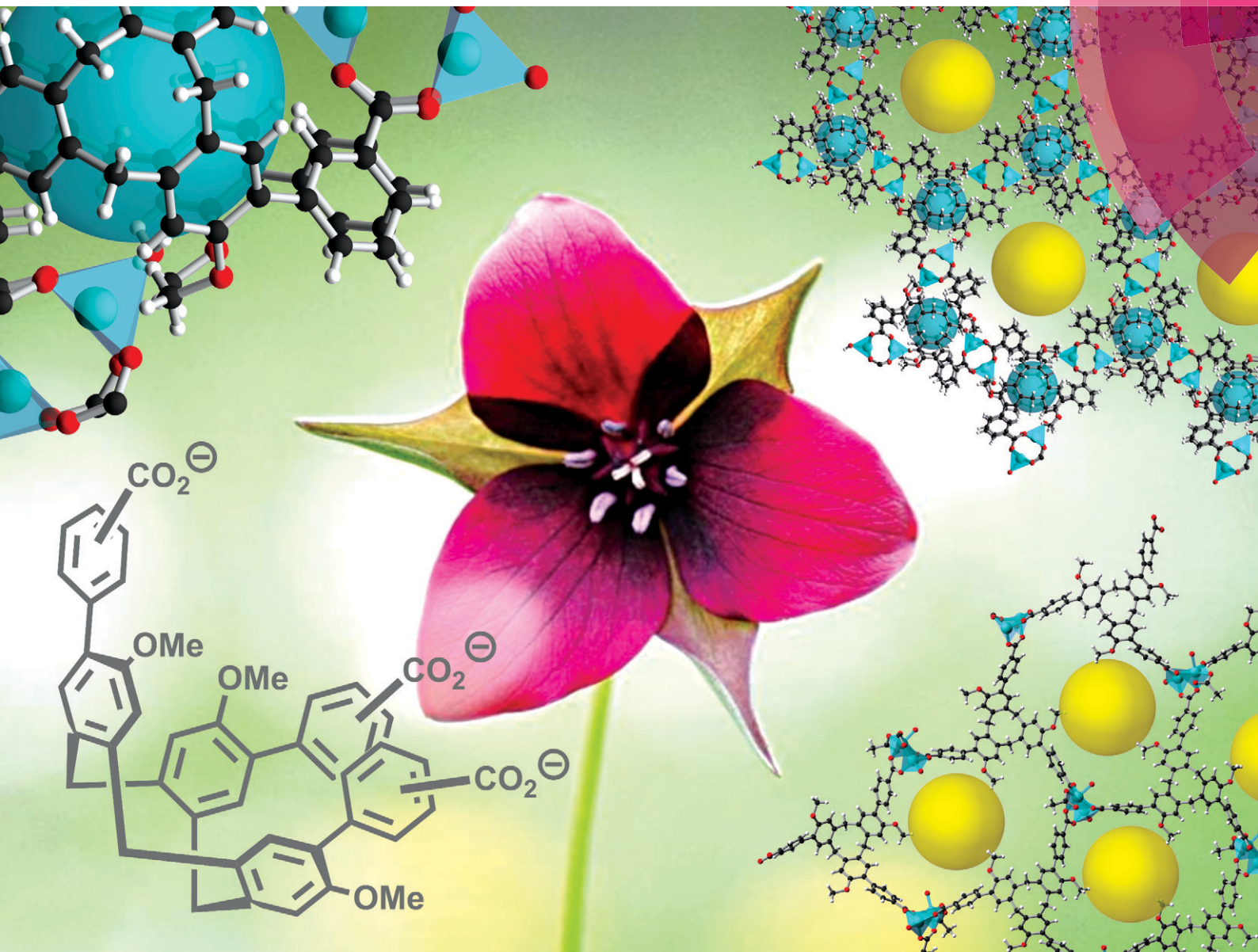


CrystEngComm

rsc.li/crystengcomm



ROYAL SOCIETY
OF CHEMISTRY

COMMUNICATION

Timothy L. Easun, Martin Schröder *et al.*

The effect of carboxylate position on the structure of a metal organic framework derived from cyclotrifluoromethane



Cite this: *CrystEngComm*, 2017, 19, 603

Received 9th September 2016,
Accepted 1st October 2016

DOI: 10.1039/c6ce01965j

www.rsc.org/crystengcomm

Two cyclotrimeratrylene-based ligands H_3L^1 and H_3L^2 have been synthesised using microwave heating and used in the formation of **1** $[Zn_2(L^1)(DMA)_2(CH_3COO)_2]$ and **2** $[Zn_6(L^2)_4(DMA)_6(H_2O)_5]$ ($DMA = N, N$ -dimethylacetamide). **1** displays an unusual trigonal paddlewheel node geometry, while $Zn^{(II)}$ paddlewheels are observed in **2**. However, the stacking of CTV molecules in **1** is replaced by an uncommon molecular capsule structure in **2**.

Introduction

Controlling self-assembly in the solid state is one of the major goals of crystal engineering. A variety of methods have been employed to achieve this aim, including ligand substitution, metal coordination, hydrogen bonding and solvent selection.^{1–5} Of these, ligand substitution or alteration can result in dramatically different structures under the same conditions of self-assembly. Specifically, the position of a substituent on an aromatic substrate can result in significantly different properties of the resultant compounds, with perhaps the best example of this being the xylenes, where the position of the methyl groups on the benzene ring gives differences in boiling point, viscosity and crystal structure.⁶

One area where systematic substitution of functional groups is hugely important is that of supramolecular self-assembly, in which complex structure and function arise during materials synthesis from often delicately balanced structural and electronic factors.⁷ This approach is particularly common in the synthesis of coordination polymers and the asso-

ciated sub-discipline of metal organic frameworks (MOFs). MOFs are crystalline microporous materials that are attractive targets for applications such as carbon capture and molecular separation due to the wide variety of linkers and metal node geometries that can be exploited.^{8–13} Here, a change in the position of a functional group such as a carboxylate can result in a completely different structure as a result of the changed connectivity of the organic linker. This has been observed for numerous linkers, ranging from simple substrates such as benzoic or pyridinecarboxylic acids^{14–17} to more complex molecules such as porphyrinic macrocycles.^{18,19}

Macrocycles such as porphyrins,²⁰ calixarenes,²¹ crown ethers^{22,23} and cyclodextrins²⁴ have been used as ligands for the formation of MOFs. However, due to the increased complexity associated with such substrates, this is a relatively underexplored area. The use of macrocycles as linkers offers advantages such as a higher density of functional sites per molecule and additional coordination sites such as hydrophobic pockets or ion binding regions, when compared to simpler substrates. Cyclotrimeratrylenes (CTVs) are one such class of bowl-shaped macrocycles containing a shallow, hydrophobic pocket and an upper rim which can be functionalised in a number of ways.²⁵

Whilst initial research into CTVs focused on their ability to bind fullerenes,^{26,27} more recently the supramolecular chemistry and metal coordination abilities of CTVs have been explored, with a diverse range of metal-organic polyhedra based upon the CTV scaffold reported.^{28–33} A few examples of coordination polymers based upon CTVs have also been reported, including low dimensional coordination polymers with lanthanide ions,³³ a covalent organic framework (COF) based upon a triformal CTV derivative³⁴ and a MOF featuring one of the ligands used in this study, (L^1)^{3–}, coordinated to a copper node, giving rectangular one-dimensional pores.³⁵

Here, we report the synthesis of the linkers H_3L^1 and H_3L^2 , in which a cyclotrimeratrylene scaffold is functionalised with *para* and *meta*-benzoic acid group, respectively. Notably,

^a School of Chemistry, The University of Nottingham, University Park, Nottingham, NG7 2RD, UK

^b School of Chemistry, The University of New South Wales, Sydney, NSW, 2052, Australia

^c School of Chemistry, Cardiff University, Main Building, Park Place, Cardiff, CF10 3AT, UK. E-mail: EasunTL@cardiff.ac.uk

^d School of Chemistry, University of Manchester, Oxford Road, Manchester, M13 9PL, UK. E-mail: M.Schroder@manchester.ac.uk

[†] Electronic supplementary information (ESI) available. CCDC 1470195–1470197. For ESI and crystallographic data in CIF or other electronic format see DOI: 10.1039/c6ce01965j

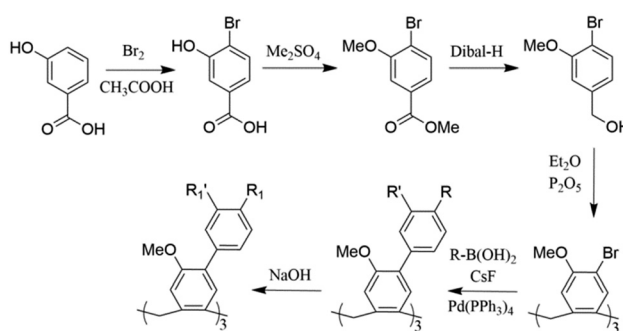


using a microwave Suzuki coupling procedure, we are able to achieve greater yields and shorter reaction times than those previously reported for Suzuki couplings involving CTVs as a substrate.³⁶ We have used these linkers in solvothermal reactions and confirm that the structures of the materials obtained are strongly dependent on the position of the carboxylate. For the *para* benzoic acid-substituted $\mathbf{H}_3\mathbf{L}^1$, a columnar stacking of CTV molecules is observed. However, the change in directionality provided by the *meta* benzoic acid component in $\mathbf{H}_3\mathbf{L}^2$ results in the formation of a molecular capsule arrangement which has not been observed previously for coordination polymers.

Experimental section

Tribromocyclotriphosphazene (CTV-Br₃) was prepared from 3-hydroxybenzoic acid in 15% yield according to a literature procedure,³⁷ and this compound was used as the substrate for Suzuki couplings. Couplings were performed under an inert atmosphere using a microwave reactor at 100 °C for 30 min, with 5 mol% Pd(PPh₃)₄ as catalyst with cesium fluoride and six equivalents of *x*-ethoxycarbonylphenylboronic acid (*x* = 4 for $\mathbf{H}_3\mathbf{L}^1$, 3 for $\mathbf{H}_3\mathbf{L}^2$). Following purification and hydrolysis of the ester groups (full experimental details can be found in the ESI†), $\mathbf{H}_3\mathbf{L}^1$ and $\mathbf{H}_3\mathbf{L}^2$ were obtained as racemic mixtures in 75% and 58% yield, respectively (Scheme 1).

The complex **1-Zn** was obtained by solvothermal reaction of $\mathbf{H}_3\mathbf{L}^1$ with Zn(NO₃)₂·6H₂O in a solvent mixture of *N,N*-dimethylacetamide (DMA) and ethanol (2.5:1) in the presence of acetic acid at 90 °C. Upon cooling and filtration, colourless needles suitable for X-ray diffraction analysis were obtained. **1** was obtained as isostructural cobalt(II) and zinc(II) complexes, **1-Zn** and **1-Co**, respectively. However only **1-Zn** will be discussed here in detail. **2-Zn** was synthesised in a similar manner but in the absence of acetic acid, where after cooling and filtration, colourless hexagonal plates of suitable quality were obtained for X-ray diffraction studies. The addition of acetic acid to this second solvothermal reaction mixture resulted in no crystalline material being produced.



Scheme 1 Synthesis of $\mathbf{H}_3\mathbf{L}^1$ and $\mathbf{H}_3\mathbf{L}^2$ starting from 3-hydroxybenzoic acid. For \mathbf{L}^1 , $R = \text{COOEt}$, $R_1 = \text{COOH}$, $R' = R_1' = \text{H}$. For \mathbf{L}^2 , $R' = \text{COOEt}$, $R_1' = \text{COOH}$, $R = R_1 = \text{H}$.

Results and discussion

1-Zn crystallises in the orthorhombic space group *Pbca*, with the asymmetric unit containing one molecule of [L¹]³⁻, two Zn(II) ions, two coordinated DMA solvent molecules and an acetate molecule (Fig. 1a), giving an empirical formula of [Zn₂(L¹)(DMA)₂CH₃COO]. The acetate molecule is coordinated to Zn(II) in a bidentate fashion, and in the absence of acetic acid no crystalline material is formed. This suggests that the acetate molecule plays an important role in the stabilisation of this particular crystal phase.

In **1-Zn**, the two Zn(II) metal centres display different coordination environments. One metal centre has a distorted tetrahedral geometry, with coordination to a solvent DMA molecule and three carboxylates from [L¹]³⁻ molecules. The other Zn(II) cation possesses a distorted octahedral geometry, with coordination to a solvent molecule and three carboxylates in

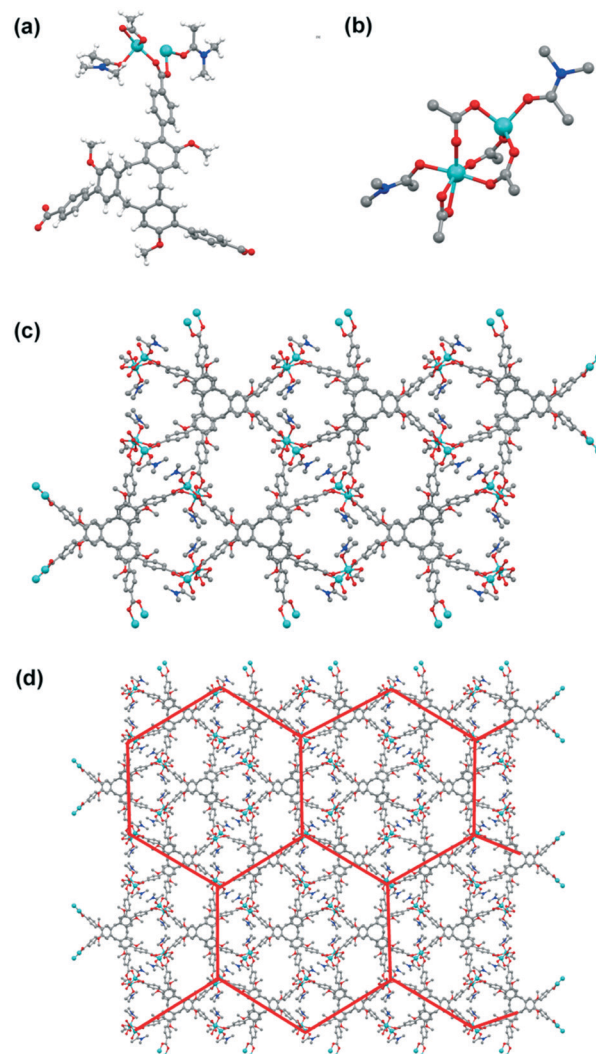


Fig. 1 View of the asymmetric unit of **1** (a), metal node geometry of **1** displaying a trigonal paddlewheel (b), three different types of channels in **1** as viewed down the *b* axis (c), and hexagonal superstructure of channels outlined in red (d). Hydrogen atoms in b-d have been omitted for clarity.



addition to a bidentate acetate molecule (Fig. 1b). Together, this arrangement of metal centres can be thought of as an asymmetric trigonal paddlewheel, where on one side, in addition to an axial solvent (in this case DMA) molecule, there is bidentate coordination to an acetate. Trigonal paddlewheel structures are uncommon,^{38–40} and this is the first example of a metal organic framework containing a metal node bearing this trigonal paddlewheel geometry.

The molecules of $[L^1]^{3-}$ stack in a columnar arrangement, with a distance of 4.9 Å between hydrophobic CTV pockets. This motif is commonly observed in crystal structures of molecular CTV-based species,^{28–30} presumably because it maximises the π – π interactions between CTV cores. In the columnar arrangement in this structure, left and right handed molecules of $[L^1]^{3-}$ stack alternately. This reduces any steric hindrance associated with extending the CTV cores through the addition of the benzoic acid moiety.

When viewed down the *b* axis, three types of channels are visible: a rhombic channel (8.65 × 9.97 Å), a pentagonal channel (5.68 (pentagon base width) × 12.63 (width of channel at its widest point) × 13.43 (channel height) Å) and a hexagonal channel (12.30 × 13.89 Å) (Fig. 1c). The rhombic channel is occupied by two solvent molecules and the pentagonal channel by two solvent molecules and two acetate molecules, but the hexagonal channel remains free of any coordinated solvents. Using a 1.2 Å probe, the solvent accessible volume for this structure is calculated to be 5.5% using the Mercury program from the CCDC software package,⁴¹ which is solely due to the unoccupied hexagonal pores. During this calculation, metal coordinated solvent molecules were not removed. When viewed down the *b* axis, a hexagonal superstructure composed of four of each type of channel is visible, with each side being approximately 22 Å (Fig. 1d).

Compound 2-Zn crystallises in the triclinic space group $P\bar{1}$, with the asymmetric unit containing four molecules of $[L^2]^{3-}$, six Zn(II) cations, six molecules of DMA and five water molecules (Fig. 2a), thus yielding a product of formula $[Zn_6(L^2)_4(DMA)_6(H_2O)_5]$. Unlike the reaction with $[L^1]^{3-}$, in the presence of acetic acid the reaction of $[L^2]^{3-}$ with Zn(II) af-

fords no crystalline material in our hands. The arrangement of the CTV ligands in 2-Zn is distinctly different to that observed in 1-Zn; a molecular capsule arrangement of $[L^2]^{3-}$ ligands is observed in 2-Zn, with no stacking interactions observed between CTV ligands in this structure. The molecular capsules are connected to each other through four-blade Zn(II) paddlewheels, as opposed to the trigonal paddlewheel structure observed for 1-Zn. The zinc paddlewheels are axially coordinated by one water molecule and one DMA molecule, with two unbound DMA molecules found inside each molecular capsule, and one addition DMA molecule *exo* to the capsules.

A capsular arrangement of CTVs in the solid state is uncommon, and although some examples have been shown for cyclotriicatechylene (CTC),^{42,43} the only examples reported for CTV-based structures incorporate complementary binding groups at their upper rim.^{44,45} In this structure, each molecular capsule is composed of one left handed and one right handed $[L^2]^{3-}$ ligand, and when viewed down the *c* axis it can be seen that these capsules pack into a hexagonal arrangement (Fig. 2b), with one molecular capsule positioned at each corner of the hexagon. These hexagons stack in an alternating *abab* manner, which reduces the available porosity for this structure. However, the solvent accessible volume was calculated to be 21%, which is markedly higher than that for 1-Zn (which is 5.5%). This is due to the presence of two types of rectangular pores in 2-Zn of dimensions 7.57 × 6.28 Å and 12.55 × 10.57 Å (Fig. 2c), as well as the interior of the capsules.

It can be seen that in the structures of 1-Zn and 2-Zn there is a balance between the preferred ligand geometry for the CTV ligand. In 1-Zn the CTV molecules stack on top of one another to maximise π – π interactions, with a preferred metal node geometry incorporating a trigonal Zn(II) paddlewheel. It has been observed previously that minor differences in ligand substitution, either from the addition of a phenyl or methyl group to an aromatic core, or through post-synthetic modification, can result in significant differences in separation behaviour, proton conductivity or dye adsorption in the resulting frameworks.^{46–48}

For the case of the *para* benzoic acid appended CTV, $[L^1]^{3-}$, the stacking interactions between CTV molecules are more favoured than the formation of four-blade Zn(II) paddlewheels. This results in the formation of an unusual trigonal paddlewheel metal node, where each Zn(II) cation in the paddlewheel has a different coordination number. This is in contrast to the previously reported MOF using this ligand,³⁵ where $[L^1]^{3-}$ is connected through Cu(II) paddlewheels (where the copper displays octahedral coordination) and a five-coordinate, square bipyramidal Cu(II) to form rectangular, one dimensional nanotubes. In that structure, no stacking of the CTV molecules is observed.

For 2-Zn, the formation of the four-blade Zn(II) paddlewheel structure is more favoured, resulting in an uncommon molecular capsule arrangement for the *meta* benzoic acid appended CTV, which results in a higher level

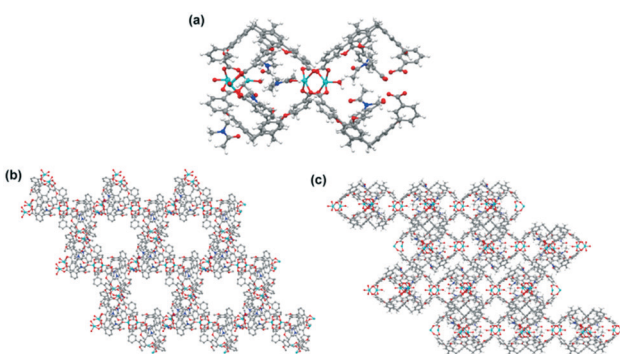


Fig. 2 View of the asymmetric unit of 2 (a), hexagonal arrangement of molecular capsules as viewed down the *c* axis (b) and two types of rectangular pores in the structure as viewed down the *a* axis (c). Hydrogen atoms and uncoordinated solvent molecules in *b* and *c* have been removed for clarity.

of porosity. As the reaction conditions in both cases are almost identical, it must be concluded that it is the position of the carboxylic acid which plays the major role determining the structural outcome of the synthesis.

Conclusions

In this work we have synthesised the *para* and *meta* benzoic acid appended cyclotrimeratrienes H_3L^1 and H_3L^2 , respectively, through a microwave assisted Suzuki coupling reaction. The use of microwave irradiation affords markedly faster reaction times and greater yields when compared with previously reported syntheses. We then used these ligands in solvothermal reactions with $Zn(NO_3)_2$ to give the corresponding coordination polymers **1-Zn** and **2-Zn**. For both of these frameworks, it can be seen that there is a finely balanced compromise between optimal ligand packing and metal node geometry. For **1**, the common CTV packing motif is observed where CTV molecules stack on top of one another, which results in an unusual trigonal paddlewheel metal node geometry. For **2-Zn**, the common four-blade paddlewheel geometry is seen, although this yields an uncommon molecular capsule arrangement of the CTV ligand. Thus, we have confirmed that the position of the carboxylic acid, here *meta* or *para*, plays a critical role in the assembly of CTV-based MOFs. This is important for the future design of porous materials based upon macrocyclic scaffolds, where maintaining porosity and functionality is crucial.

Acknowledgements

We thank the EPSRC for support. MS gratefully acknowledges support from the ERC for an Advanced Grant. TLE gratefully acknowledges the Royal Society for the award of a University Research Fellowship. ADM thanks the Australian Government for the award of an NHMRC-ARC Fellowship (APP1106751).

References

- 1 H. Furukawa, K. E. Cordova, M. O'Keeffe and O. M. Yaghi, *Science*, 2013, **341**, 974.
- 2 C. L. Jones, A. J. Tansell and T. E. Easun, *J. Mater. Chem. A*, 2016, **4**, 6714–6723.
- 3 W. Lu, Z. W. Wei, Z. Y. Gu, T. F. Liu, J. Park, J. Tian, M. W. Zhang, Q. Zhang, T. Gentle, M. Bosch and H. C. Zhou, *Chem. Soc. Rev.*, 2014, **43**, 5561–5593.
- 4 Y. J. Cui, Y. F. Yue, G. D. Qian and B. L. Chen, *Chem. Rev.*, 2012, **112**, 1126–1162.
- 5 D. J. Tranchemontagne, J. L. Mendoza-Cortes, M. O'Keeffe and O. M. Yaghi, *Chem. Soc. Rev.*, 2009, **38**, 1257–1283.
- 6 J. Fabri, U. Graeser and T. A. Simo, *Xylenes: Ullman's Encyclopedia of Industrial Chemistry*, Wiley-VCH, Weinheim, 2000.
- 7 L. Chen, Q. Chen, M. Wu, F. Jiang and M. Hong, *Acc. Chem. Res.*, 2015, **48**, 201–210.
- 8 Z. C. Hu, B. J. Deibert and J. Li, *Chem. Soc. Rev.*, 2014, **43**, 5815–5840.
- 9 J. W. Liu, L. F. Chen, H. Cui, J. Y. Zhang, L. Zhang and C. Y. Su, *Chem. Soc. Rev.*, 2014, 6011–6081.
- 10 Y. B. He, W. Zhou, G. D. Qian and B. L. Chen, *Chem. Soc. Rev.*, 2014, 5657–5678.
- 11 Y. Yoon, K. Suh, S. Natarajan and K. Kim, *Angew. Chem., Int. Ed.*, 2013, **52**, 2688–2700.
- 12 X. J. Zhang, W. J. Wang, Z. J. Hu, G. N. Wang and K. S. Uvdal, *Coord. Chem. Rev.*, 2015, **284**, 206–235.
- 13 M. C. So, G. P. Wiederrecht, J. E. Mondloch, J. T. Hupp and O. K. Farha, *Chem. Commun.*, 2015, **51**, 3501–3510.
- 14 L. B. Handy, P. R. Raithby, L. H. Thomas and C. C. Wilson, *New J. Chem.*, 2014, **38**, 2135–2143.
- 15 S. Mirtschin, E. Krasniqi, R. Scopelliti and K. Severin, *Inorg. Chem.*, 2009, 6375.
- 16 X. L. Wu, N. N. Ding, W. H. Zhang, F. Xue and T. S. A. Hor, *Inorg. Chem.*, 2015, **54**, 6680–6686.
- 17 P. Teo and T. S. A. Hor, *Coord. Chem. Rev.*, 2011, **255**, 273–289.
- 18 D. Feng, W. C. Chung, Z. Wei, Z. Y. Gu, H. L. Jiang, Y. P. Chen, D. J. Daresbourg and H. C. Zhou, *J. Am. Chem. Soc.*, 2013, **135**, 17105–17110.
- 19 S. Lipstman and I. Goldberg, *Cryst. Growth Des.*, 2013, **13**, 942–952.
- 20 A. Fateeva, P. A. Chater, C. P. Ireland, A. A. Tahir, Y. Z. Khimyak, P. V. Wiper, J. R. Darwent and M. J. Rosseinsky, *Angew. Chem., Int. Ed.*, 2012, **51**, 7440–7444.
- 21 G. L. Zheng, G. C. Yang, S. Y. Song, X. Z. Song and H. J. Zhang, *CrystEngComm*, 2014, **16**, 64–68.
- 22 D. E. Lim, S. A. Chyun and M. P. Suh, *Angew. Chem., Int. Ed.*, 2014, **53**, 7819–7822.
- 23 T. H. Chen, A. Schneermann, R. A. Fischer and S. M. Cohen, *Dalton Trans.*, 2016, **45**, 3063–3069.
- 24 R. A. Smaldone, R. F. Forgan, H. Furukawa, J. J. Gassensmith, A. M. Z. Slawin, O. M. Yaghi and J. F. Stoddart, *Angew. Chem., Int. Ed.*, 2010, **49**, 8630–8634.
- 25 M. J. Hardie, *Chem. Soc. Rev.*, 2010, **39**, 516–527.
- 26 M. J. Li, C. H. Huang, C. C. Lai and S. H. Chiu, *Org. Lett.*, 2012, **14**, 6146–6149.
- 27 E. Huerta, G. A. Metselaar, A. Fragoso, E. Santos, C. Bo and J. de Mendoza, *Angew. Chem., Int. Ed.*, 2007, **46**, 202–205.
- 28 J. J. Henkelis, C. J. Carruthers, S. E. Chambers, R. Clowes, A. I. Cooper, J. Fisher and M. J. Hardie, *J. Am. Chem. Soc.*, 2014, **136**, 14393–14396.
- 29 J. J. Henkelis, J. Fisher, S. L. Warriner and M. J. Hardie, *Chem. – Eur. J.*, 2014, **20**, 4117–4125.
- 30 C. J. Sumby and M. J. Hardie, *Angew. Chem., Int. Ed.*, 2005, **44**, 6553–6557.
- 31 T. K. Ronson, C. J. Carruthers, J. Fisher, T. Brotin, L. P. Harding, P. J. Rizkallah and M. J. Hardie, *Inorg. Chem.*, 2010, **49**, 675–685.
- 32 T. K. Ronson and M. J. Hardie, *CrystEngComm*, 2008, **10**, 1731–1734.
- 33 J. J. Henkelis, T. K. Ronson and M. J. Hardie, *CrystEngComm*, 2003, **15**, 3688–3693.
- 34 J. R. Song, J. Sun, J. Liu, Z. T. Huang and Q. Y. Zheng, *Chem. Commun.*, 2014, **50**, 788–791.



35 J. T. Yu, J. Sun, Z. T. Huang and Q. Y. Zheng, *CrystEngComm*, 2012, **14**, 112–115.

36 J. T. Yu, Z. T. Huang and Q. Y. Zheng, *Org. Biomol. Chem.*, 2012, **10**, 1359–1364.

37 D. J. Cram, M. E. Tanner, S. J. Keipert and C. B. Knobler, *J. Am. Chem. Soc.*, 1991, **113**, 8909–8916.

38 I. M. Hauptvogel, V. Bon, R. Grunker, I. A. Baburin, I. Senkovska, U. Mueller and S. Kaskel, *Dalton Trans.*, 2012, **41**, 4172–4179.

39 C. A. Murillo, *Comments Inorg. Chem.*, 2015, **35**, 39–58.

40 S. I. Vagin, A. K. Ott and B. Rieger, *Chem. Ing. Tech.*, 2007, **79**, 767–779.

41 C. F. MacRae, P. R. Edgington, P. McCabe, E. Pidcock, G. P. Shields, R. Taylor, M. Towler and J. van de Streek, *J. Appl. Crystallogr.*, 2006, **39**, 453–457.

42 P. Satha, G. Illa and C. S. Purohit, *Cryst. Growth Des.*, 2013, **13**, 2636–2641.

43 P. Satha and C. S. Purohit, *Proc. Natl. Acad. Sci., India, Sect. A*, 2014, **84**, 221–225.

44 A. Westcott, J. Fisher, L. P. Harding, P. Rizkallah and M. J. Hardie, *J. Am. Chem. Soc.*, 2008, **130**, 2950–2951.

45 S. B. Lee and J. I. Hong, *Tetrahedron Lett.*, 1996, **37**, 8501–8504.

46 Y. Wu, H. Chen, D. Liu, J. Xiao, Y. Qian and H. Xi, *ACS Appl. Mater. Interfaces*, 2015, **7**, 5775–5787.

47 S. Kim, K. W. Dawson, B. S. Gelfand, J. M. Taylor and G. K. H. Shimizu, *J. Am. Chem. Soc.*, 2013, **135**, 963–966.

48 H. Hahm, S. Kim, H. Ha, S. Jung, Y. Kim, M. Yoon and M. Kim, *CrystEngComm*, 2015, **17**, 8418–8422.

